Journal of Natural Gas Science and Engineering 26 (2015) 229–239

Contents lists available at ScienceDirect

Journal of Natural Gas Science and Engineering

journal homepage: www.elsevier.com/locate/jngse

Experimental study on the probe dynamic behaviour of feeler pigs in detecting internal corrosion in oil and gas pipelines

Xiaolong Li, Shimin Zhang*, Shuhai Liu, Xiaoxiao Zhu, Kang Zhang

College of Mechanical and Transportation Engineering, China University of Petroleum – Beijing, Changping, Beijing, 102249, China

ARTICLE INFO

Article history:
Received 9 April 2015
Received in revised form
15 June 2015
Accepted 16 June 2015
Available online 23 June 2015

Keywords:
Pipeline
Feeler pig
Dynamic behaviour
Corrosion
Detection precision

ABSTRACT

Leakages are the major cause of in-service natural gas and oil pipeline accidents, and many factors, such as corrosion, can lead to leakages. The feeler pig is one of the most typical contact-testing tools in oil and gas pipelines. In this paper, the probe dynamic behaviour of the feeler pig in detecting internal corrosion has been investigated using a handmade inspecting system. The dynamic characteristics of the probe are different in the uphill section and the downhill section, and the trajectory of the probe is asymmetric. A bouncing phenomenon was found in the outlet region of the corrosion. The experimental results indicated that both the speed and the spring pre-tightening elastic force are closely related to the inspection precision. The research in this paper provides guidance for studying the inspection precision of the feeler pig.

1. Introduction

Pipelines function as blood vessels to bring such necessities as oil and natural gas, and they are considered to be the most favoured mode of transportation of gas and liquid in large quantities (Kishawy and Gabbar, 2010; Tolmasquim et al., 2008; Xiaoxiao Zhu et al., 2014; Esmaeilzadeh et al., 2009; Nguyen et al., 2001a, b). With the long timelines employed, the problem of pipeline ageing is becoming more and more serious, and pipelines aging greatly promotes defects. Among pipeline defects, corrosion is the critical factor affecting the service life of pipelines (Teixeira et al., 2008; Cosham et al., 2007; Podgorbunskikh et al., 2008; Choi et al., 2003). According to statistics by the US National Transportation Safety Board, 59% of pipeline accidents are caused by corrosion. According to the former Soviet Union pipeline accident statistics, during 1981–1987, 1210 accidents happened in the 240,000 km pipeline. Among these, accidents caused by corrosion were 45.1% of the total accidents (Tiratsoo, 1992). Therefore, regular pipeline inspection is significant, not only prolonging pipeline life but also greatly reducing the loss caused by accidents (Cosham et al., 2007; Choi et al., 2003; Kim et al., 2003a, b).

At present, many internal inspection technologies can be used to investigate pipeline defects all over the world. Depending on the different detection principles, the technology can be divided into two categories: non-destructive testing (NDT) and contact testing (CT) (Kim et al., 2003a, b; Dai et al., 2012; Carvalho et al., 2006). NDT includes ultrasonic technology (UT) and magnetic flux leakage (MFL). UT uses acoustic wave reflection to inspect corrosion, so it needs a homogeneous fluid with good acoustic properties to serve as sonic wave coupling. Because of this limitation, UT is difficult to use for inspecting gas pipelines and is mostly used in oil pipelines (Skjelvareid et al., 2013; Park,.1996; Siqueira et al., 2004). The MFL technology produces a magnetic field in the pipe wall to sense leakages inside the pipe as the wall thickness changes. Therefore, it is difficult to inspect small diameter and thick wall pipelines using MFL. Similar to UT, the biggest advantage of MFL is high inspection accuracy, but it also has disadvantages including low spatial resolution and low readability of the MFL pig report generated by "magnetic spots" (Gloria et al., 2009; Carvalho et al., 2006; Camerini et al., 2008). Furthermore, due to the limited size of the sensor, the MFL pig has difficulty going through a curved pipeline. In addition, owing to the detection principle of MFL, the pipeline needs to be degaussed when the pig sweeps across the pipeline.

Through collecting analogue signs and converting it into the angular variation of the inspection arm, the CT registers the movement process generated by internal defects and then delineates the corrosion features (Dai et al., 2012; Kim et al., 2003a, b; Camerini et al., 2008). Compared to the NDT, CT performs the direct

* Corresponding author.
E-mail address: zsm1976748@126.com (S. Zhang).

http://dx.doi.org/10.1016/j.jngse.2015.06.033
1875-5100/

List of symbols

$\overline{a_{x_0}}$	The acceleration of the barycenter moving along the horizontal direction in the downhill section
$\overline{a_{y_0}}$	The acceleration of the barycenter moving along the vertical direction in the downhill section
$\overline{a_{x_1}}$	The acceleration of the barycenter moving along the horizontal direction in the uphill section
$\overline{a_{y_1}}$	The acceleration of the barycenter moving along the horizontal direction in the uphill section
$\overrightarrow{a_{n_0}}$	Normal acceleration in the downhill section
$\overrightarrow{a_{t_0}}$	Tangential acceleration in the downhill section
$\overrightarrow{a_{n_1}}$	Normal acceleration in the uphill section
$\overrightarrow{a_{t_1}}$	Tangential acceleration in the uphill section
Δh	The depth of the defect
k	Stiffness of the spring
l	The length of the probe
n	The number of pulses
t_0	Time spent in the downhill section
t_1	Time spent in the uphill section
x_0	The distance of the probe head moving along the horizontal direction in the downhill section
x_1	The distance of the barycenter moving along the horizontal direction
x	The initial spring length
x'	The spring length corresponding to a changing angle $\Delta\alpha$
Δx	The changing spring length corresponding to a changing angle $\Delta\alpha$
y_1	The distance of the barycenter moving along the vertical direction
$E_{k_{Y1}}$	Kinetic energy of the probe along the Y direction during the bouncing of the probe
$E_{k_{Y1}}$	Kinetic energy of the probe along the negative Y direction during the bouncing of the probe
F	The spring pre-tightening force
F′	The spring force corresponding to a changing angle $\Delta\alpha$
H	The distance between the fixed bracket and the rotary table
L_0	The distance of the fixed bracket moving along the direction of the fixed bracket speed in the downhill section
L_1	The distance of the fixed bracket moving along the direction of the fixed bracket speed in the uphill section
Q	Thermal energy generated during the bouncing of the probe
S	The length of the defect in the direction of the moving probe
V	The velocity of the fixed bracket
$\overline{V_{x_0}}$	The average velocity of the probe barycenter along the horizontal direction in the downhill section
$\overline{V_{y_0}}$	The average velocity of the probe barycenter along the vertical direction in the downhill section
$\overline{V_{t_0}}$	The average velocity of the probe barycenter along the tangential direction of the trajectory in the downhill section
$\overline{V_{x_1}}$	The average velocity of the probe barycenter along the horizontal direction in the uphill section
$\overline{V_{y_1}}$	The average velocity of the probe barycenter along the vertical direction in the uphill section
$\overline{V_{t_1}}$	The average velocity of the probe barycenter along the tangential direction of the trajectory in the uphill section
W_e	Elastic energy generated during the bouncing of the probe
α	The initial angle between the fixed bracket and the probe
$\Delta\alpha$	The changing angle corresponding to the depth Δh
$\widehat{\zeta}$	The corresponding radian to rotate angle $\Delta\varphi$
δ_0	The average angular acceleration in the downhill section
δ_1	The average angular acceleration in the uphill section
$\Delta\varphi$	The corresponding rotate angle to pulse n
$\overline{\omega_0}$	The average angular velocity in the downhill section
$\overline{\omega_1}$	The average angular velocity in the uphill section
λ	The distance between the defect and the central axis of the rotary table

dimensional measurement of the pipeline internal corrosion by contact with no practical limits of wall thickness or a need for a homogeneous fluid during the inspection. CT also has an excellent ability to go through a curved pipeline. Moreover, compared to the NDT, CT has easy data post-processing and inner surface pipeline reconstruction. In addition, the cost of the CT is far lower than that of the MFL and the UT; because of these unique advantages, the CT is widely used for the internal detection of pipelines.

Based on the difference of contact arms, the product of the CT can be classified into three types: wheel, arm and probe pigs (Cox et al., 1936; Smith et al., 1990; Rosenberg et al., 1992). Among them, the probe pig is the most typical product of contact-testing and is also called the feeler pig. Compared to wheel and arm pigs, not only could a feeler pig inspect the diameter, but it could also detect and quantify internal corrosion and welds. Furthermore, the detection precision of CT is similar to the UT and MFL pig. Therefore, the feeler pig has been widely recognized in internal pipeline corrosion inspection. Fig. 1 shows the detection process of the feeler pig. Since the 1960s, the pipeline industry has been using and developing feeler pigs to inspect small diameter production

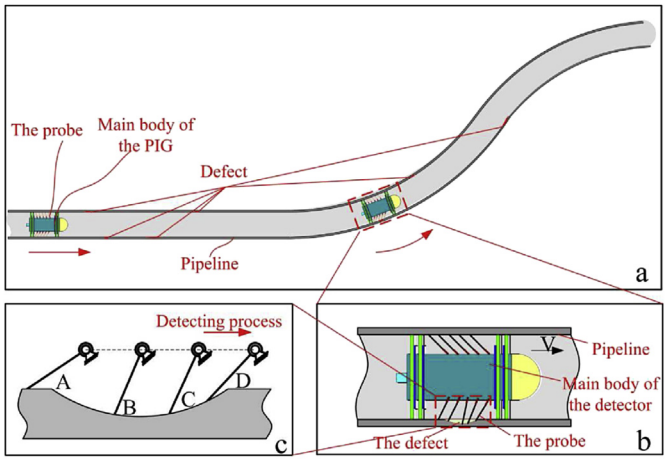

Fig. 1. Schematic diagram of the feeler pig inspection process.